

Received January 23, 2019, accepted February 18, 2019, date of current version April 3, 2019.

Digital Object Identifier 10.1109/ACCESS.2019.2901292

Fractional-Order Integration Based Fusion Model for Piecewise Gamma Correction Along With Textural Improvement for Satellite Images

HIMANSHU SINGH¹, (Student Member, IEEE), ANIL KUMAR¹, (Member, IEEE),
L. K. BALYAN¹, AND HEUNG-NO LEE², (Senior Member, IEEE)

¹Indian Institute of Information Technology, Design and Manufacturing Jabalpur, Jabalpur 482005, India

²Gwangju Institute of Science and Technology, Gwangju 500712, South Korea

Corresponding author: Heung-No Lee (himanshu.iiitj@gmail.com)

This work was supported by the National Research Foundation of Korea (NRF) Grant funded by the Korean government (MSIP) (NRF-2018R1A2A1A19018665).

ABSTRACT Fractional-order integration (FOI) and its beauty of optimally ordered adaptive filtering for image quality enhancement are latently too valuable to be casually dismissed. With this motivation, a new Riemann–Liouville fractional-order calculus-based spatial-masking methodology is proposed in this paper in association with counterbalanced piecewise gamma correction (PGC). A generalized FOI-based mask is also suggested. This mask is negatively augmented with the original image for harvesting texture-based benefits. PGC is just employed through a constructive association of both kinds of reciprocally dual gamma values ($\gamma_1 = \gamma$ and $\gamma_2 = 1/\gamma$, $\forall \gamma > 1$), which leads to optimally desired enhancement when applied in a weighted counter-correction manner. Efficiently improved and recently proposed opposition-based learning inspired sine–cosine algorithm is employed in this paper, along with a newly framed fitness function. This fitness function is devised in a novel manner by taking care of textural as well as non-textural details of the images. In this paper, especially for dark images, 130% increment is achieved over the input contrast along with the simultaneous 147% increment in the discrete entropy level and 22.8% increment in the sharpness content. Also, brightness and colorfulness are reported with 130% and 196.4% increased with respect to the input indices, respectively. In addition, the textural improvement is advocated in terms of desired comparative reduction of gray-level co-occurrence matrix-based metrics, namely, correlation, energy, and homogeneity, which are suppressed by 25.6%, 72.5%, and 21.8%, respectively. This performance evaluation underlines the excellence and robustness for imparting proper texture as well as edge preserved (or efficiently restored) image quality improvement.

INDEX TERMS Fractional-order (FO) masking filter, fractional-order integration (FOI), Riemann–Liouville (RL) definition, sine cosine algorithm (SCA), opposition-based learning (OBL), gray-level co-occurrence matrix (GLCM), quality enhancement, optimal mask designing, two-dimensional (2-D) adaptive filtering, piecewise-gamma correction (PGC).

I. INTRODUCTION

Remotely acquired digital imagery and its various forms keep on laying the core and firm foundation of today's technological era, and hence it is quite implicit that necessity and importance of quality enhancement and desired information restoration is having the prime concern. Various integers' based mathematical suggestions got appreciation in the last two decades, but fractional-order calculus-based

mathematical advancements in image processing applications are still fascinating in one form or the other. Fractional-order calculus (FOC) is a kind of eternal source of analytical processing power. FOC [1], [2], since the historical day of its paradoxical invention, evolved from a very popular Leibniz–L'Hôpital technological conversation, as on September 30, 1695; the theory is still gloriously blooming day-by-day for drawing significant application based consequences. FOC is now being more widely accepted in current technological trends. The involvement of classical, as well as integer-based calculus in anthropological scientific advancement,

The associate editor coordinating the review of this manuscript and approving it for publication was Sara Dadras.

is indispensable. Hence, it is very hard to say about “fractional-order or non-integral order calculus” even after 323 years of discussion and its consequent advancement, that in which domain of science and technology, FOC is incapable to facilitate the corresponding technological advancement. FOC has recently been applied in various areas of engineering, science, finance, applied mathematics, and bio-engineering with its remarkable success. Contemporary advancements in all technological spheres for social welfare cannot be imagined without signals and their “on-demand or application-specific “contextual processing, in one form or the other. A large amount of work has already been focused on image enhancement through FO differentiation based masking [3]. More robustness can be imparted for pre-existing methodologies by an organized and efficient involvement of swarm intelligence in association with the fractional-differential approach. Now through this paper, it’s the time of debut for fractional-order integral based adaptive filtering for image quality enhancement. With such an objective, an interesting approach is proposed by suggesting a fusion based framework by employing optimally ordered fractional-order integration for gamma corrected image enhancement application for almost all kind of images.

Fundamentally, image visualization characteristics can be categorized as spectral, textural and contextual features for almost all kinds of remotely sensed images. Spectral features account for general tonal variations corresponding to each band in the visible and/or infrared region of the electromagnetic spectrum. Structural variation and corresponding inter as well as intra-organization of the contextual surfaces of the images can be better identified as the texture of the image. Texture, in one form or the other, accounts for most of the information related to all kinds of preprocessing tasks associated with remotely sensed imagery. It is also responsible for identifying the objects or regions of interest in an image. Also, intensity levels and their sharpness also contribute to overall behavioral characteristics of the image. Hence, in general, quality enhancement can be seen as collective coordination of improved spatial, contextual, textural and edge-dependent image features. Initially, for various years, the histogram of the acquired image has been utilized for image enhancement.

Initially, researchers got highly fascinated by histogram equalization (HE) based approaches, especially, general histogram equalization (GHE). GHE flattens and enlarges the dynamic range of image’s histogram by remapping the gray but its performance is inadequate due to the issue of mean-shift and also, it is quite unable to preserve the local spatial features of an image [4]. Due to this, the sole attention of the researchers got shifted to histogram-distribution along with local histogram modifications, and also towards their corresponding advantages. Therefore, several algorithms were developed for image enhancement based on local histogram modifications. Later on, median-mean dependent sub-image-clipped HE (MMSICHE) [5] was proposed for image enhancement along with further bisecting both of sub-histograms on the basis of the median count of the

corresponding pixels in both sub-histograms. Contrast limited adaptive histogram equalization (CLAHE or ADAPHE [6]), has been also proposed as a very efficient variant of GHE. ADAPHE operates on small regions in the image in a tile-wise manner rather than the entire image. Later all neighboring tiles are combined using 2-D bilinear interpolation to eliminate artificially induced boundaries.

Blind-reliability over HE (local and global both) based enhancement approaches is not advisable because of their tendency to impart uniform intensity distribution without knowing the behavior of input image; and hence, gamma correction based methods were suggested by various researchers for contrast enhancement. Gamma correction was initially applied directly on image pixels in its original domain. Afterward, transform domain gamma correction based on wavelets and filter-banks based transformations were suggested with a common problem of manual tuning for the desired and relevant gamma value which is a very tedious and a trivial kind of task. It was found that applying gamma correction through histogram is easier and quite efficient rather than applying gamma correction directly on the corresponding image itself. Later on, adaptive gamma correction with weighting distribution (AGCWD) [8] and its various effectively improved versions like [9]; were better performed for this objective, where desired contrast enhancement is imparted by utilizing a gamma value-set of size 2^{L-1} for a corresponding L bit image, which itself is derived by using cumulative distribution of the intensity values present in low contrast input image.

The averaging histogram equalization (AVHEQ) approach [7] was proposed by combining linear color channel stretching, histogram averaging, which is followed by consequent one to one mapping of the intensity levels. In the same context, HE based optimal profile compression (HEOPC) [10] and HE with maximum intensity coverage (HEMIC) [11] were proposed, where the objective is to harvest more and more intensity levels in an exhaustive manner. Afterward, the intensity and edge-based adaptive unsharp masking filter (IEAUMF) [12] based enhancement have been also proposed by employing the unsharp masking filter for edge augmentation. Although, these approaches are focused over the harvesting of more and more intensity levels which generally leads to kind of smoothening and hence, improvement of textural details is not focused on it, and sometimes leads to the unbalanced exposure also.

Most of the methodologies are based on parallel pipelined methods by framing collective coordination of various efficient operations. Most of the conventional methodologies are based on histogram redistribution mechanism, in one way or the other. Usually, histogram-redistribution doesn’t care much about textural details. Also, the spatial pixel-wise orientations are not considered while (one-dimensional) histogram based processing. A second serious issue is the appearance of saturation effects in case of gamma correction which leads to over-enhancement and under-exposed patches in the enhanced version of the image. Both of these issues are tried

to be rectified, as in the proposed approach, gamma correction is employed in a counter-correction based balanced manner by involving both gamma expanded and gamma compressed channels. Piecewise gamma correction (PGC) is proposed in an effective manner by suggesting a fusion based framework by the constructive involvement of reciprocal gamma values which leads to interim compressed as well as interim expanded images. This is initially proposed as a dual correction for GHE and termed as PGC based HE (PGCHE) where the results are not so enriched due to lack of textural treatment. So, it was further improved for PGC based textural enhancement by taking the benefits of positive augmentation through fractional order differentiation based adaptive filtering. Later, it is found more effective than in place of FOD based masking, if unsharp masking is modified by applying fractional order integration based adaptive filtering in a negative augmentation manner, the outcomes are much better.

In this manuscript, idea is to introduce the benefits of FOI based adaptive two-dimensional filtering for overall textural and non-textural benefits. In addition, parallel “FOI based textural improvement and edge restoration” is also suggested. The prime contribution in this manuscript is an inclusion of highly adaptive, multidimensional optimally weighted framework through association of piecewise gamma correction along with the fractional-order integration based negatively augmented unsharp masking for texture highlighted, overall quality enhancement for remotely sensed imagery. An opposition based learning inspired sine-cosine algorithm based optimization mechanism termed as OBL-SCA model is framed in accordance with the concerned tuning problem for free parameters; utilizing a newly framed objective function which is designed by using intensity-dependent and GLCM based fidelity parameters. The fitness function is specially framed by considering textural and illumination improvement for dark images. As, FO masking is itself not sufficient for dark images, hence, for proper exposure shift, counter-balanced piecewise gamma correction is also entangled with it. Hence, idea is to employ gamma correction in a dual manner by constructive fusion of PGC through employing gamma correction in a dual manner by a constructive amalgamation of interim channels.

In this context, reciprocally dual values of gamma are utilized for employing the desired enhancement. The closed form pre-existing approaches are usually unable to serve the purpose efficiently. Hence, a constructive combination of artificial intelligence or machine learning inspired optimization principles along with classical optimization approaches can be applied. Particle Swarm Optimization (PSO) [13], Artificial Bee Colony (ABC) optimization [14], Moth-Flame Optimization (MFO) [15], Sine Cosine Algorithm (SCA) [16], etc. have been also developed by imitating various nature-inspired analogies. In general, most of such kinds of optimization strategies are suffering from common issues of local trapping, which can be eradicated efficiently if governed by some kind of artificial learning based intelligence.

Considering the above key-points in mind, sine-cosine optimizer using opposition-based learning [17] is integrated with the proposed framework. In this manner, better converging behavior is proposed by planning a gradient-based exploration and exploitation.

The core contribution for achieving overall quality enhancement, in this manuscript can be point-wise identified as:

- A novel framework of FOI based masking is proposed for adaptive image filtering which leads to analogous FO unsharp masking.
- Collective benefits of newly identified PGC and FO integral are justified and proposed in this paper for textural improvement along with on-demand dual gamma-correction.
- In one manner, textural and non-textural content of the image is separately processed as per the “on-demand” basis and later an optimally framed fusion is employed for collective contribution.
- A newly framed fitness function or the cost function is formulated for deciding the tuning parameters to make the approach highly adaptive for a diverse blend of images.
- This newly proposed cost function is designed by blending the significant fidelity parameters in an effective and robust manner for highlighting the effective convergence of the algorithm.

The remaining manuscript is drafted as follows: after brief literature survey and basic introduction in section 1; section 2 explains the problem formulation; section 3 explains the proposed Piecewise Gamma Corrected (PGC) RL-FOI based Masking (PGCRLFOIM) algorithm followed by its stepwise framework. Later, section 4 deals with the experimentation followed by corresponding results and discussion; and in section 5, conclusions are drawn.

II. PROBLEM FORMULATION

The central idea is to impose both of these corrections on the fractionally masked and negatively augmented image which is just an analogy of negative augmentation of the fractionally derived low pass filtered/smoothed intensity channel. Thus, sharpness behavior of the texture and edge content can be highlighted and finally corrected through a reciprocal set of gamma values in a dual balanced manner. Hence, both of these individually account for keeping the processed intensity channels in the permissible intensity ranges in a constructive manner and hence, fruitful exploration for all of the intensity values can be done, by proper avoidance for the saturation due to an accumulation of the pixel values in extreme-end bins of the histogram. Hence, information loss can be minimized by avoidance of over-saturated patches as well as improperly exposed regions. Thus, an attempt is made for the proposal of a complete framework is by collective contribution of textural, spectral and contextual base quality improvement. Hence, successful harvesting of the optimal masking which is analogs to low pass filtering of fractional order and its

negative augmentation leads to a kind of adaptive enhancement based masking which is later counter corrected by both gamma values by collective piecewise contribution of both values of reciprocal gamma set ($\gamma_1 = \gamma$ and $\gamma_2 = 1/\gamma$, $\forall \gamma > 1$), and thus leads to interim enhanced and interim compressed gamma value set.

III. PROPOSED METHODOLOGY

Fundamental instinct behind this approach is to design an efficient and highly adaptive behavior-dependent end-to-end optimal framework for overall image quality improvement. Both the textural as well as non-textural image details are managed along with proper edge restoration. A generalized N-ordered FOI based mask framing strategy is suggested using rotation-invariant uniformity principle; so that, whenever it is assimilated along with piece-wise gamma correction, it leads to better quality improvement for the texture of the poorly-illuminated digital image. Usually, remotely sensed, imperfectly illuminated satellite images come under this category; however, this proposed framework is also applicable for other similar kinds of rich-grained images.

A. PIECEWISE GAMMA CORRECTION

Piecewise gamma correction (PGC) is applied by an optimal evaluation of gamma-compressed and corresponding gamma-expanded channel. It should be notified that both of these counter-gamma values are reciprocal of each other and hence, advantageous for lower-end as well as higher-end intensity correction. This, in turn, results into restriction of oversaturated as well as sub-enhanced patches and hence, the objective of more and more information exploration get fulfilled. When intensity values of the input image (I_{in}) are normalized from zero to unity, if they are exponentially employed by a gamma value more than unity, it leads to intensity compression and hence, can be termed as gamma compressed intensity channel (I_{gcp}) as [2], [3]:

$$I_{gcp} = (I_{in})^\gamma, \quad \gamma > 1, \quad (1)$$

Correspondingly, its dual can be evaluated by the reciprocal of the gamma value as in Eq. (1). It leads to shifting towards the dark end of the histogram's abscissa, and hence, leads to a compressed kind of intensity distribution. Such interim channel is utilized basically for imparting counter correction for over-enhanced or saturated bright patches. Complimentary to this, as per the Eq. (2), the intensity values of the input channel get shifted towards the bright end of the histogram's abscissa. Hence, it leads to expansion of intensity distribution towards the bright end. This leads to counter correction for dark patches and also for boosting up for less illuminated image-patches. The interim gamma corrected expanded (I_{gex}) channel can be evaluated as [2], [3]:

$$I_{gex} = (I_{in})^{1/\gamma}, \quad \gamma > 1, \quad (2)$$

B. RL FRACTIONAL ORDER INTEGRATION

For adaptive kind of isolation of non-textural ingredients from the image in highly optimal fashion, benefits of the FOI are derived by following the Euclidean domain based RL definition for FOI. This is analogously derived from integer based fundamentals. Originally inspired by the Cauchy integration for the concerned analytic function, primarily for any complex plane; symbolically it can be justified as [1]:

$$D^n f(t) = \frac{1}{(n-1)!} \int_a^t (t-u)^{n-1} \cdot f(u) du, \quad n \in \mathbb{N} \quad (3)$$

Thus, according to the RL definition, as suggested, the Cauchy integral formula can be directly extended to enter the fractional-order calculus domain. By convention, it is required that $f(t)$ must be a causal function. In other words, $f(t)$ must identically be vanishing for $t < 0$, which occurs intuitively, by default, in case of digital images, since negative pixel intensities are insignificant. From the standard formalization of ν -ordered RLFOI for any function $f(t)$ in the interval $[0, t]$ and $[-\infty, t]$ as follows:

$$J^\nu f(t) = \frac{1}{\Gamma(\nu)} \int_{-\infty}^t (t-u)^{\nu-1} \cdot f(u) du, \quad \nu > 0, \quad (4)$$

The duration of signal $f(t)$ is $[0, t]$ and $\Gamma(\cdot)$ is the Gamma Function defined as:

$$\Gamma(z) = \int_0^\infty e^{-t} t^{z-1} dt, \quad (5)$$

Discrete-time equivalent of J^ν can be derived by framing a discrete time FO kernel $I^\nu(n)$ as:

$$I^\nu(n) = \begin{cases} \frac{n^{\nu-1}}{\Gamma(\nu)}, & n > 0 \\ 0, & n \leq 0 \end{cases}, \quad (6)$$

$$A = I^\nu(1); B = I^\nu(2); C = I^\nu(3); D = I^\nu(4); E = I^\nu(5); \quad (7)$$

$$\begin{aligned} & [A, B, C, D, E, \dots] \\ & = \left[\left(\frac{1^{\nu-1}}{\Gamma(\nu)} \right), \left(\frac{2^{\nu-1}}{\Gamma(\nu)} \right), \left(\frac{3^{\nu-1}}{\Gamma(\nu)} \right), \left(\frac{4^{\nu-1}}{\Gamma(\nu)} \right), \dots \right], \quad (8) \end{aligned}$$

C. PROPOSED PGCRIFOI FRAMEWORK

Rather than following the image-dependent FO differential masking based edge-augmentation concept (as earlier proposed by the same authors), the idea is to suppress the non-textural details first, which is followed by overall boost up of the processed image. Thus, the local spatial intensity saturation, as well as over-brightness enhancement, can be counter-attacked. For this purpose, the RL-FOI based odd-dimensional symmetric mask is framed in a generalized manner. To avoid the further higher order complexity, a 5×5 sized mask is derived by following the fundamental FO integral

calculus. In addition, the mask coefficients are arranged to maintain the proposed mask rotational invariant. The conceptual analysis is to suppress the non-textural content of the image first; and then, enhancement for the resulted image in a fashion so that PGC can be imposed in an optimal manner. Fractional-order 1-D filtering can be extended to a 2-D image matrix, and hence, a set of fractional-order partial differential equations w.r.t. x and y-direction can be expressed as [3]:

$$\begin{aligned}
 I_{x^v}^v f(x, y) &\approx \left(\frac{1^{v-1}}{\Gamma(v)}\right) \cdot f(x, y) + \left(\frac{2^{v-1}}{\Gamma(v)}\right) \cdot f(x-1, y) \\
 &+ \left(\frac{3^{v-1}}{\Gamma(v)}\right) \cdot f(x-2, y) + \dots + \left(\frac{(n+1)^{v-1}}{\Gamma(v)}\right) \\
 &\cdot f(x-n, y), \tag{9}
 \end{aligned}$$

$$\begin{aligned}
 I_{y^v}^v f(x, y) &\approx \left(\frac{1^{v-1}}{\Gamma(v)}\right) \cdot f(x, y) + \left(\frac{2^{v-1}}{\Gamma(v)}\right) \cdot f(x, y-1) \\
 &+ \left(\frac{3^{v-1}}{\Gamma(v)}\right) \cdot f(x, y-2) + \dots + \left(\frac{(n+1)^{v-1}}{\Gamma(v)}\right) \\
 &\cdot f(x, y-n), \tag{10}
 \end{aligned}$$

An RL definition based FO 5x5 mask is created by maintaining a similar kind of gradient behavior in almost all eight directions. These directions can be viewed w.r.t. the center pixel based balanced orientation at angles of 0, 45°, 90°, 135°, 180°, 225°, 270°, 315° and 360°, respectively. In this work, the behavior of smoothing filter or blurring image filter is extended by framing this FO low pass filter kind of mask. The elements of this 5x5 mask are normalized so that sum of all elements remains unity. Masks of 3x3 and 7x7 size have been also tested for this, but a trade-off is settled for 5x5 size. Integer-ordered masks are usually employed for detection of the smooth content of images by complete exclusion of major and minor edges. This extent of inclusion or exclusion depends on the order of FOI mask which itself acts as a 2-D adaptive filter to extract the low-frequency content of the image under consideration. Idea is to extract the non-edge content of the image optimally based on the adaptively decided order, and finally, deduct this information content from the input image. The later emphasis on the whole image leads to a highlighted textural content of the image. Masking is employed through a symmetric mask using only the first three coefficients as shown in Eq. (11). Fundamentally, 2-D linear filtering is done by convolving these filters from left to right for all rows individually and then by convolving these filters from top to bottom for all columns, similarly.

$$H_x = H_y = \frac{0.125}{(A+B+C)} \begin{pmatrix} C & 0 & C & 0 & C \\ 0 & B & B & B & 0 \\ C & B & 8A & B & C \\ 0 & B & B & B & 0 \\ C & 0 & C & 0 & C \end{pmatrix}, \tag{11}$$

It has to be taken care that, size of the convolved product must be the same as the size of input image channel matrix. FO changes and correspondingly adaptive nature of these masks can be identified through the spectral behavior for these masks more precisely. Next step is to compute the fractional-order integration based negatively augmented masking for deriving a third interim channel, which is a texture improved version of the input channel. This analogy is inspired from unsharp masking mechanism, with its negatively augmented version and hence, resembles the suppressed low pass filtered version of the image by optimally ordered version of the FOI by following its RL definition. This interim channel is evaluated as:

$$I_{fimf} = I_{in} + k \cdot \lambda \cdot (I_{in} - I_v), \tag{12}$$

2-D convolutional filtering of the input channel (I_{in}) by employing the RL FOI mask (H) can be understood as:

$$I_v = H \otimes I_{in}, \tag{13}$$

Later on, k which is the scaling factor for adaptive augmentation (can be assumed 0.5). In order to accomplish the design objective, a hyperbolic profile, λ is adopted, as:

$$\lambda = 0.5 [1 + \tanh(3 - 6(|I_v| - 0.5))], \tag{14}$$

The profile is decided by an adaptive contribution of the magnitude of negatively augmented; FOI based filtered channel's pixels at the corresponding image coordinate. Here, $\tanh(\pm 3) = \pm 0.995 \approx 1$ is sufficient to approximate a unity scale. The rationale in defining the input based profile also applies here. Since the corresponding magnitudes are bounded between ± 1 , a modification is made as $6 \times (|I_v| - 0.5)$ in order to bind the profile coefficients within ± 3 . The multiplication by 6 is used as a normalization accounting for the doubled edge magnitudes due to the possible two edge or textural polarities. An enhanced version of the image can be evaluated by weighted and collective fusion of all three interim enhanced images. The parameters p and q are solely responsible for the weighted amalgamation of these channels, as:

$$I_{en} = \left(\frac{p}{1+q}\right) \cdot I_{gcp} + \left(\frac{1-p}{1+q}\right) \cdot I_{gex} + \left(\frac{q}{1+q}\right) \cdot I_{foimf}, \tag{15}$$

Balanced benefits of both gamma compression and gamma expansion over the image under consideration in a reciprocally framed counter-correction manner; and hence, for weighted involvement in a pixel-wise augmentation manner, the parameter p is introduced for imparting intensity exposure based enhancement. Later on, for textural and edge improvement, a novel FOI based negative augmentation scheme is suggested and hence, in accordance with it, third interim channel is also framed. Further, its weighted involvement is also a matter of prime concern, and hence, the parameter q is involved. The role of the q must be framed in such a manner that a balanced involvement for gamma corrected interim channels along with the proposed

negatively augmented RL-FOI mask based filtered interim-channel I_{foimf} can be framed. Thus, collective involvement of texture enhanced version along with rest of the channels is premier concern and hence, a highly balanced provision is made for it as follows. Here, the gamma value is kept more than unity and hence, its reciprocal leads to value in the range (0, 1]. Balanced and weighted framework contribution of all interim channels can be maintained by keeping the value of p in the range of [0, 1] and q can be varied throughout the positive range. Assuming a case when $q \rightarrow 0$ it leads to the ignorance or absence of texture improved channel and such type of situation arises when the acquired image is of smooth nature. Contrary to this, a larger value of q stands for highly textured images. When, q is unity, it indicates half of the contribution is due to the presence of I_{foimf} and remaining both gamma based channels are confined to rest of the half share. According to above justification, q must be varied in the range [0, ∞), but while looking for its practical aspect, it can be noticed that beyond the range of [0, 4), there is a significant drop in contribution as it will be below 20%, and hence, ignored in this work. Now, the third parameter i.e. gamma (γ) value must be positively varied starting from the unity. Hence, when it is simply unity, it leads to simple unity scaled one-to-one mapping. When raised above unity value, it leads to counter related gamma-compressed and gamma-expanded interim channels. Very high gamma value obviously leads to unnatural artifacts and hence, just for avoiding such kind of scenario, range of the gamma parameter is confined to (1,3), which is experimentally found suitable w.r.t. both gamma-corrected and gamma-expanded channels. Next, to frame the influence of the fractional-order for corresponding fractional-order integration, ν is varied in the range of (0,1) so that accordingly adaptive mask can be framed. In this way, now this problem can be easily identified as an optimization problem for search in a four-dimensional search space for positive exploration and exploitation. Finally, it can be simply identified that all four parameters (p , q , γ , and ν) have to be varied in the range [(0,1),[0,4),[1,3),(0,1)], respectively.

D. FITNESS FUNCTION FORMULATION

Mostly the objective functions have been framed by considering only the entropy of the content in the mind. In this formulation, both kinds of discrete entropy contents (intensity based as well as GLCM based entropy values (i.e., DE_O and DE_{GLCM}) for the processing image is considered. To better highlight the effectiveness of the edges as well as the texture content of the images, special considerations are framed by proposing a novel objective function in this context. Magnitude gradient matrix for the output image (GM_O) is evaluated for the processed image by employing the Sobel-Feldman operator along the rows as well as columns of the image. Summing up all of the pixel-wise gradient's magnitude implies the sharpness or the edgy content of the image. This kind of summing-up may lead to a higher order magnitude. For this purpose, a logarithmic operation is

imparted twice over this sum to make it up to the comparable order. Along with it, normalized image contrast measure is also amalgamated by considering its exponential treatment for making it in a comparable order. Cube root for the product of these three quantities made this expression equivalent to the order for the other term in the expression namely, colorfulness metrics' enhancement factor which is just a ratio of colorfulness measure for the output image to the colorfulness measure for the input image. Also, to introduce sufficient dominance of entropy content, the exponential of the framed fraction is implied. As a whole, a newly introduced fitness-function in the proposed enhancement algorithm, is designed as (16), as shown at the bottom of the next page:

E. REINFORCEMENT LEARNING BASED SINE-COSINE OPTIMIZER

Remembering the well-known and remarkable applicability along with the keen understanding for No-free lunch theory, it can never be obvious that, "which evolutionary and/or metaheuristic algorithm will perform best, when associated with the proposed framework". It's again a very challenging to decide that, which optimization mechanism is more effective when associated with the proposed framework and hence, various algorithms (like, PSO, ABC, CSO, SCA, MFO, OBL-SCA, etc.) have been tested for this purpose. Finally, OBL-SCA is found performing very efficiently. Initially, a trigonometrically inspired stochastic population-based optimization, termed as Sine-Cosine Algorithm was suggested. For more optimal behavior, this mechanism is efficiently modified through reinforcement learning. Thus, the opposition based learning inspired Sine-Cosine Algorithm (OBL-SCA) came into existence. Here, OBL-SCA is incorporated in a well-framed manner for obtaining the desired level of quality enhancement in association with the proposed framework. In this context, both the fine as well as coarse texture should be restored and enhanced along with their contrast and entropy enhancement. Fundamentally, SCA is based on sine and cosine based trigonometric functions those are responsible for exploration and exploitation in the search space. A machine learning strategy termed as opposition based learning (OBL) is incorporated along with SCA, so that its intelligence for exploration as well as exploitation mechanism can be utilized, and the search-space can be explored in a more appropriate manner. While evaluating the cost function, the OBL leads to the best solution-set among the original as well as its opposite position data-set, collectively; and hence, this intelligent step-wise learning mechanism finally leads to early convergence. Similar to most of the population-based optimization approaches, initially, a set of randomly evaluated solutions is created in this approach. On repeated consecutive evaluations in a similar fashion, this random set is improved by imparting a set of certain sine-cosine based trigonometric rules, which is the core of this optimization approach. Obviously, the optimal solution hunt is never guaranteed in a single run execution for population-based techniques. Nevertheless, with appropriate population

size of search agents in fixed iteration counts, the probability of attaining global optimum solution can be increased. Irrespective of the behavior of stochastic population-based optimization approaches, the major effort distribution can be categorized into two phases, like exploration versus exploitation. Eventually, in the exploration phase, a high-level abrupt randomness is imparted to find the more and more promising regions of the search space as a set of random solutions. Contrary to this, in the exploitation phase, steady changes are framed for various random solutions, and consequently, the random variations are made noticeably less. The above-mentioned phases can be inherently characterized by following a set of position updating expressions, as follows:

$$X_i^{t+1} = X_i^t + r_1 \cdot \sin(r_2) \times |r_3 \cdot P_i^t - X_i^t|, \quad (17)$$

$$X_i^{t+1} = X_i^t + r_1 \cdot \cos(r_2) \times |r_3 \cdot P_i^t - X_i^t|, \quad (18)$$

where, X_i^t stands for the current position of the solution at t^{th} iteration correspondingly in the i^{th} dimension. The randomness of the exploration phase is maintained by employing four random variables, namely, r_1, r_2, r_3 and r_4 . The usage selection for both of the above equations, is separately governed by r_4 , and hence, it is random and equi-probable. P_i^t stands for i^{th} dimension's destination point for the corresponding t^{th} iteration. Above expressions behave somehow in conjugate fashion, merged using a uniformly distributed random variable r_4 in the range of $[0,1]$.

$$X_i^{t+1} = \begin{cases} X_i^t + r_1 \cdot \sin(r_2) \cdot |r_3 \cdot P_i^t - X_i^t|, & r_4 < 0.5, \\ X_i^t + r_1 \cdot \cos(r_2) \cdot |r_3 \cdot P_i^t - X_i^t|, & r_4 \geq 0.5, \end{cases} \quad (19)$$

The above equation expresses the core updating mechanism ensuring both exploration as well as exploitation collectively. The random parameter r_1 governs the direction of movement. The direction can be inside or outside the region covering the solution to destination intermediate distance. r_2 symbolizes the magnitude of the corresponding to and fro shift. Also, the random variable r_3 is associated for imparting weight randomly for the drift towards the destination and hence, stochastic behavior can be introduced. The corresponding net effect is emphasized if $r_3 > 1$, and deemphasized if $r_3 < 1$. At last, the parameter r_4 is solely responsible for switching exchange in-between the sine and cosine based conjugate equations. The engagement of sine and cosine expressions while framing the behavior of position updating equations, leads to the term ‘‘Sine Cosine Algorithm’’ (SCA) for this approach. It can be easily understood that the entire interim space between two solutions can be defined through the above equations. It should be easily noticed that higher dimensional equivalent system can also be realized, similarly in the corresponding

Algorithm 1 Sine Cosine Algorithm

- 1: **Initialize** a set of search agents (solutions)
 - 2: **Repeat**
 - 3: Compute the values for all search agents by employing the proposed cost function
 - 4: Update solution set by using the best achieved values so far ($P = X^*$)
 - 5: Update the random variable vector r_i ($\forall i \in 1$ to 4)
 - 6: Update the current search agents' position through Eq. (19)
 - 7: **until** ($t <$ maximum iteration count)
 - 8: **Return** the best found solution till the maximum count of iterations and consider it global optimum solution
-

hyper-plane. The conjugate behavior along with the cyclic or periodic nature for sine and cosine functions influences the re-allocation of intermediate or local solutions and hence, following it, better exploration can be easily achieved. Also, for exploring the outside region i.e. between the corresponding destinations can be done by just changing the range of these trigonometric expressions. The relative as well as absolute change of range of sine and cosine expressions leads to relative updating of the position outside/inside the interim region in-between itself and another solution. The above mentioned random position is characterized by r_2 defined in the range $[0, 2]$ employed through updating the equation. Hence, this mechanism ensures the collective effect of exploration as well as exploitation of the entire search space for corresponding dimension iteratively. It is the promising intellectual behavior to maintain the balance of exploration and exploitation, which highlights the outperformance of this optimizer. In this context, assuming a constant positive integral damping factor (a), for the t^{th} iteration, the random variable r_1 is defined in a linearly reducing fashion using the follow expression as:

$$r_1 = a(1 - t/T), \quad (20)$$

where, t signifies the current iteration, and T stands for the total iteration count. The resultant damping or range-reduction during the consecutive course of iterations can be easily understood as an effect of r_1 over the employed updating equation. Also, it can be noticed that the Sine Cosine optimizer explores efficiently, when sine and cosine function ranges in $(1, 2]$ and $[-2, 1)$. Correspondingly, the search space is exploited efficiently when sine and cosine ranges in $[-1, 1]$. The pseudo-code can be understood as a sequence of updating equations employed iteratively by evaluating all four kinds of random parameters. The core algorithm preserves the best achieved solution so far, and this solution is further identified as a destination point in the next step for

$$J \triangleq \left(\frac{CM_O}{CM_I} \right) + \sqrt[3]{e^{SDO} \cdot (DE_O + DE_{GLCM}) \cdot \left(\log \log \left(\sum_{m=1}^M \sum_{n=1}^N (GM_O(m, n)) \right) \right)}, \quad (16)$$

TABLE 1. Information regarding test satellite images.

Image S. No.	Geo-Spatial Location	Spatial Dimensions	Satellite Sensor	Pixel Resolution
1.	Brussels, Belgium [18]	1655 X 1128	QuickBird	0.65m
2.	Himalaya Range [19]	2000 X 1137	Pleiades-1A	0.5m
3.	Millau Viaduct, France [20]	2000 X 2000	Pleiades-1B	0.5m
4.	Guam - Mangilao Golf Resort [18]	2430 X 2488	QuickBird	0.65m
5.	Riyadh, Saudi Arabia [18]	1461 X 1352	QuickBird	0.65m
6.	Los Angeles, California [18]	3500 X 3341	QuickBird	0.65m

Algorithm 2 OBL-SCA Approach

- 1: Define variables
1. Defining upper and lower bounds
2. Initialize a set of search agents X (solutions)
3. Evaluate the opposite ensemble X' as: $\bar{X} = \{\bar{x}_{ij}\} = \{u_i + l_i - x_{ij}\}$, $i = 1, 2, 3, \dots, N$. Where, x_{ij} and \bar{x}_{ij} denote the i^{th} point of the j^{th} solution of x and its corresponding
4. Choose the best N solutions from combined population-set ($X \cup \bar{X}$).
5. Identify this solution set as input for further steps.
6. Repeat
7. Compute the values for all search agents by employing the proposed cost function
8. Update the solution set by using the best achieved values so far ($P = X*$)
9. Update the random variable vector r_i ($\forall i \in 1$ to 4)
10. Update the current search agents' position
11. **until** ($t < \text{maximum iteration count}$)
12. **Return** the best found solution till the maximum count of iterations and consider it global optimum solution

updating other variables w.r.t. it. With the increasing iteration count, range of sine and cosine functions is updated to emphasize the better exploration. The termination of sine-cosine optimizer is executed as the maximum iteration count is achieved. The smooth transition switching in-between exploration and exploitation phases is the best intellectual feature of this approach due to adaptive range selection for sine and cosine functions. Also, the best global optimal approximation achieved till the current iteration is considered as the destination for drifting; and hence, the chances of getting lost of the search agents during optimization, is efficiently suppressed. SCA also leads to the abrupt changes initially and gradual changes in later stages. Step-wise, proposed approach and hereby employed algorithms are as follows:

IV. EXPERIMENTATION AND DISCUSSION

Experimental validation along with comparative performance evaluation is done by reimplementation of various state-of-the-art methods such as GHE, MMSICHE [5], ADAPHE [6], AVHEQ [7], AGCWD [8], HEOPC [10], HEMIC [11], IEAUMF [12], PGCHE [4] and PGCDFM [3]. Qualitative

Algorithm 3 Proposed PGCRLFOIM Framework

- 1: **INPUT (1)** : Input image (I_{in})
- 2: **INPUT (2)**: $X = \{p, q, \gamma, v\}$ as the input parametric vector consisting of weighting parameters (p, q) gamma value (γ) order of fractional-order integral mask (v) scaling parameter for negative augmentation (k).
- 3: **OUTPUT**: GLCM based cost function (J) and Quality Improved Output Image (I_{en})
- 4: Evaluation of the tile-wise equalized (I_{teq}) input channel.
- 5: Computation of gamma compressed interim intensity channel
- 6: Computation of gamma expanded interim intensity channel
- 7: Evaluation of v -ordered FOI mask (H) as suggested in eq. (11).
- 8: Fractionally ordered filtering is imparted through these masks to extract non-textured information as, $I_v = I_{in} \otimes H$
- 9: Computation of partially texture enhanced interim image by employing: $I_{foim} = I_{in} + 0.5.\lambda (I_{in} - I_v)$.
- 10: Computation of the enhanced image using Eq. (15),
- 11: Evaluation of the cost function, as shown in Eq. (16),
- 12: **RETURN**: Magnitude of the cost function J .

and quantitative outcomes for the enhanced images for various methods are also presented in this paper. For quantitative assessment and corresponding qualitative analysis, visually improved and resultant images obtained by employing a variety of state of the art methodologies can be collectively evaluated in Fig. 1-6. In the similar manner, corresponding tabular evaluation is also presented in Table 2, by assembling most significant eight fundamental performance measures for all of the state-of the art methodologies published recently. Various satellite images acquired from standard databases (as listed in Table 1) are tested. Especially, to make the images dark and low contrasted, a fixed intensity value is deducted from these test images and hence, substantial information content is initially loosed. Later, through proper experimentation the information regain is attained. In this manner, a kind of assurance/confidence is achieved that, the proposed framework will be well suited for the required enhancement of the remotely sensed, poorly illuminated satellite images.

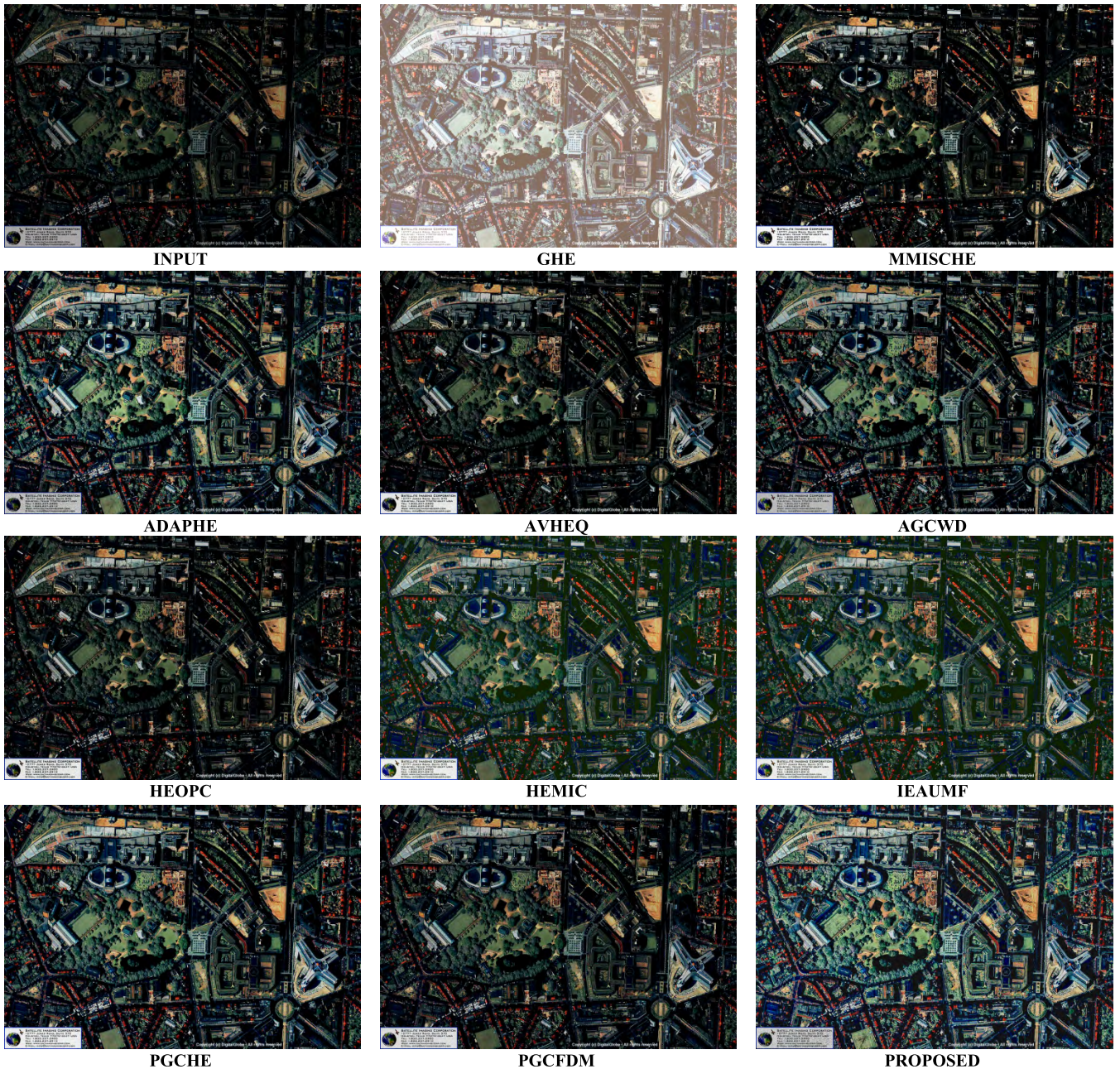


FIGURE 1. Visual presentation/ qualitative evaluation with comparison among input images; GHE; MMSICHE; ADAPHE; AVHEQ; AGCWD; HEOPC; HEMIC; IEAUMF; PGCHE; PGCDFM and the proposed approach for Image 1 (i.e., Brussels, Belgium).

A. BASIS FOR COMPARATIVE EVALUATION

Eight highly reliable and fundamentally identified measures, namely brightness (B), contrast (V), discrete Shannon entropy (H), sharpness (S), colorfulness (C), GLCM-correlation (GC), GLCM-energy (GE), and GLCM-homogeneity (GH) are employed here for explicit measurement for the excellence over various methodologies. Quality improvement can be justified by relative increment in B, V, H, S, and C along with relative decrement in GC, GE, and GH.

B. ONE-DIMENSIONAL HISTOGRAM BASED PERFORMANCE INDICES

Brightness (or mean, B) value for M by N sized image matrix $I(m,n)$ is evaluated as an averaged summation, as:

$$Brightness(B) = \frac{1}{M \times N} \sum_{m=1}^M \sum_{n=1}^N I(m,n), \quad (21)$$

Average intensity spread or the variance (V) accounts for the image contrast, responsible for a naturally pleasant look, can

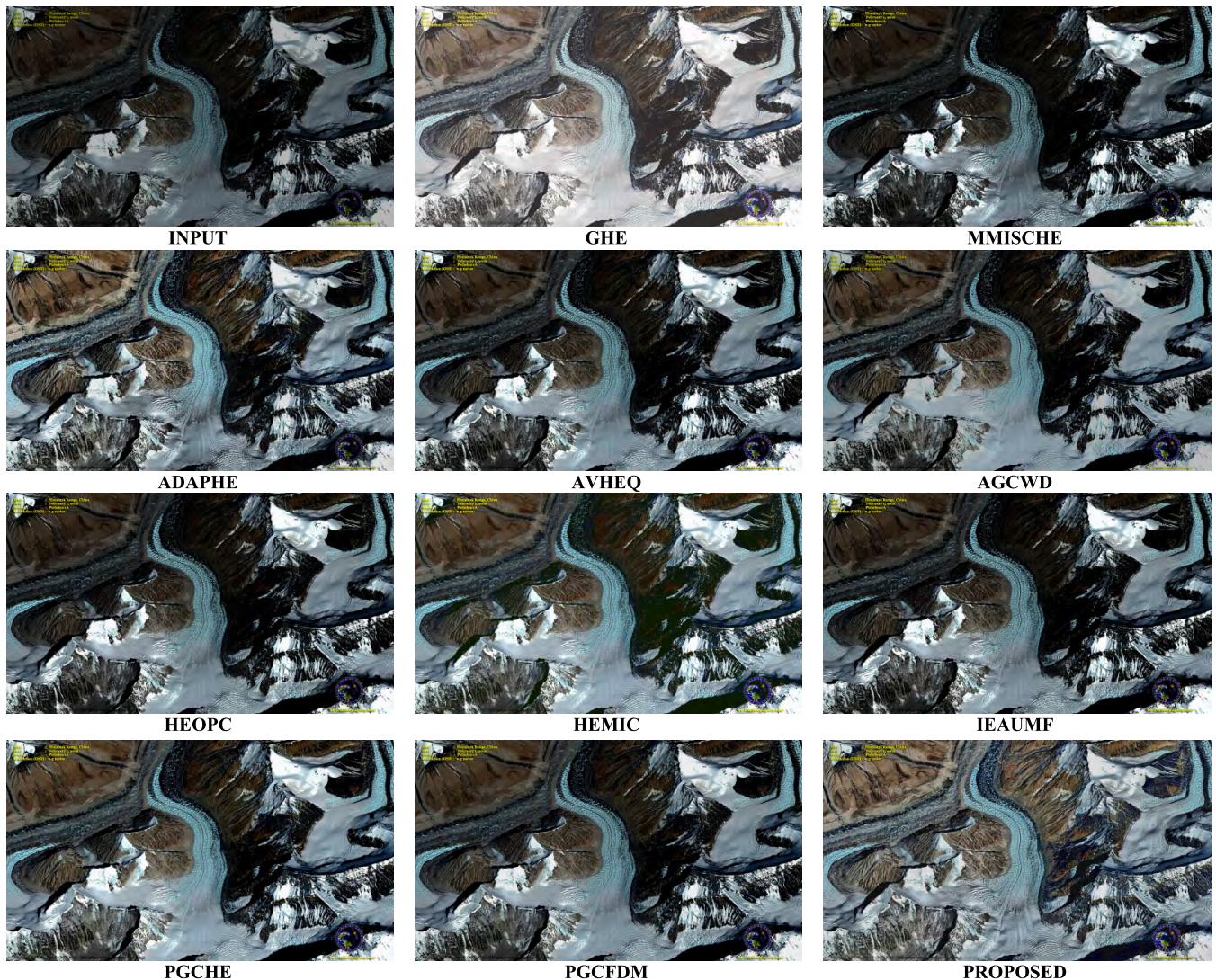


FIGURE 2. Visual presentation/ qualitative evaluation with comparison among input images; GHE; MMSICHE; ADAPHE; AVHEQ; AGCWD; HEOPC; HEMIC; IEAUMF; PGCHE; PGCDFM and the proposed approach for Image 2 (i.e., Himalaya Range).

be evaluated as:

$$Contrast (V) = \frac{1}{M \times N} \sum_{m,n} I(m, n)^2 - \left(\frac{1}{M \times N} \sum_{m,n} I(m, n) \right)^2, \quad (22)$$

Information content is quantified by Shannon entropy of the image and hence, bounded probability calculation using normalized image histogram, as:

$$Entropy (H) = - \sum_{i=0}^{I_{max}} p_i \log_2(p_i), \quad (23)$$

where, $p_i = n_i / (M * N)$ accounts for the intensity level-wise possibility of occurrence and, maximum intensity level is symbolized by I_{max} . Accountability for the presence of the edge content can be easily identified through the sharpness content of the image that can be also identified as the gradient

of the image, evaluated as:

$$Sharpness (S) = \frac{1}{M \times N} \sum_{m,n} \left(\sqrt{\Delta m^2 + \Delta n^2} \right), \quad (24)$$

where, $\Delta m = I_{enh}(m, n) - I_{enh}(m + 1, n)$ and $\Delta n = I_{enh}(m, n) - I_{enh}(m, n + 1)$ symbolizes for the accountability of the local values of gradient content of the image. For color images, color channel's coordination is also significant. Thus, utilizing relative colors' variance and relative colors' mean value, coordination of different color channels can be identified as 'colorfulness' of the image, which can be evaluated as,

$$Colorfulness (C) = \sqrt{\sigma_{rg}^2 + \sigma_{yb}^2} + 0.3 \sqrt{\mu_{rg}^2 + \mu_{yb}^2}, \quad (25)$$

$$\Delta rg = R - G; \Delta yb = 0.5 (R + G) - B; \quad (26)$$

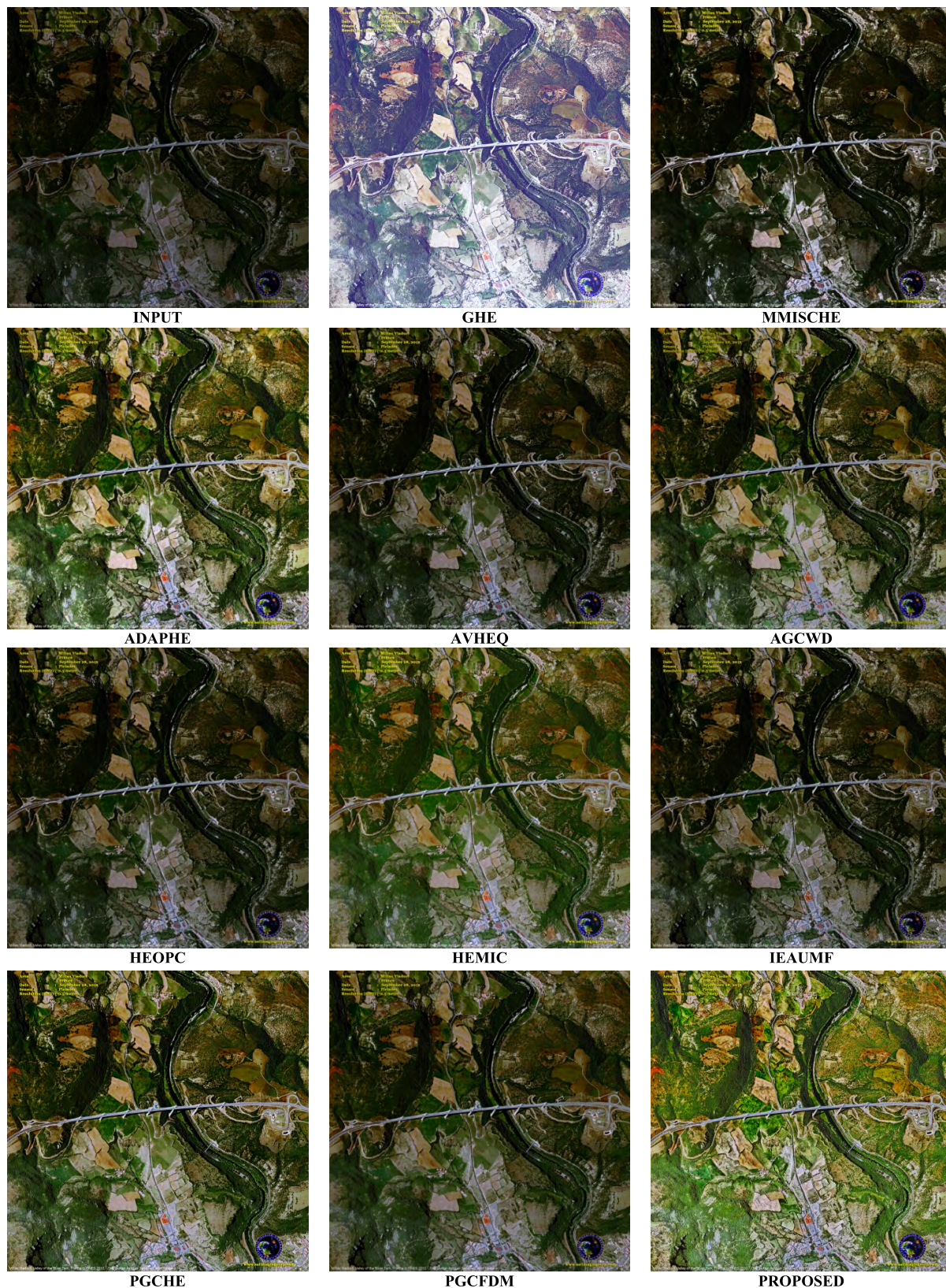


FIGURE 3. Visual presentation/ qualitative evaluation with comparison among input images; GHE; MMSICHE; ADAPHE; AVHEQ; AGCWD; HEOPC; HEMIC; IEAUMF; PGCHE; PGCFDMF and the proposed approach for Image 3 (i.e., Millau Viaduct, France).

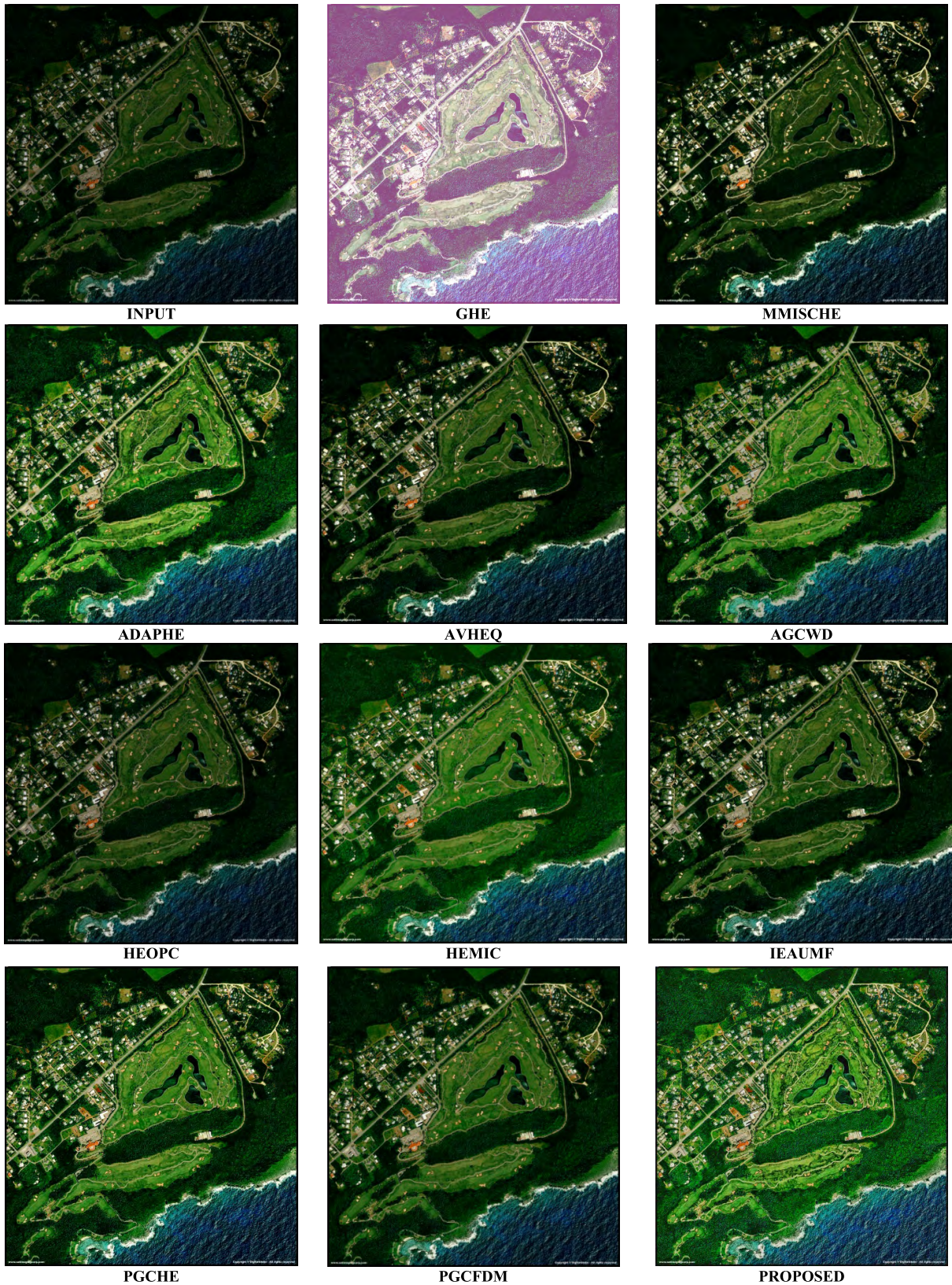


FIGURE 4. Visual presentation/ qualitative evaluation with comparison among input images; GHE; MMSICHE; ADAPHE; AVHEQ; AGCWD; HEOPC; HEMIC; IEAUMF; PGCHE; PGCDFM and the proposed approach for Image 4 (i.e., Guam - Mangilao Golf Resort).

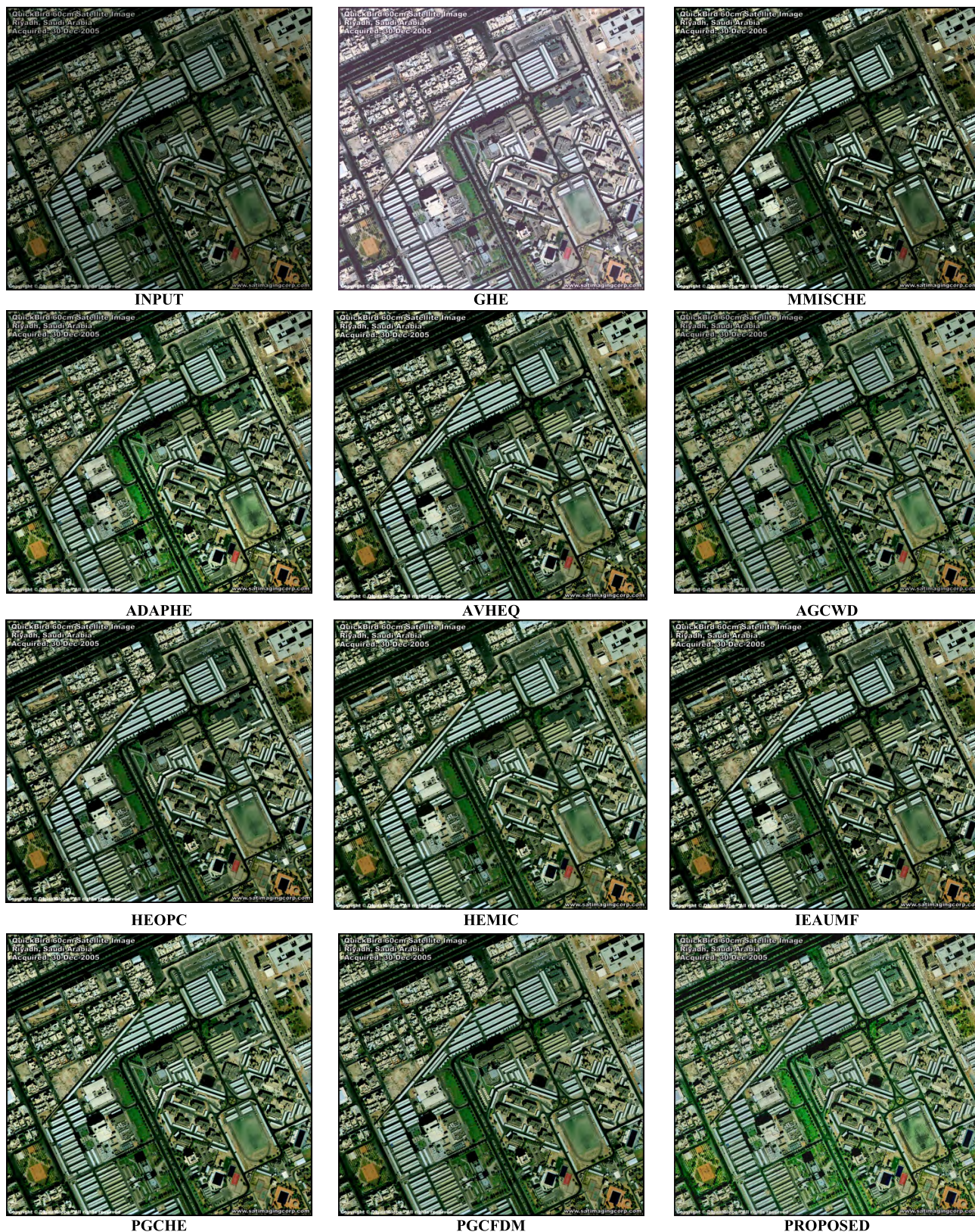


FIGURE 5. Visual presentation/ qualitative evaluation with comparison among input images; GHE; MMSICHE; ADAPHE; AVHEQ; AGCWD; HEOPC; HEMIC; IEAUMF; PGCHE; PGCDFM and the proposed approach for the Image 5 (i.e., Riyadh, Saudi Arabia).

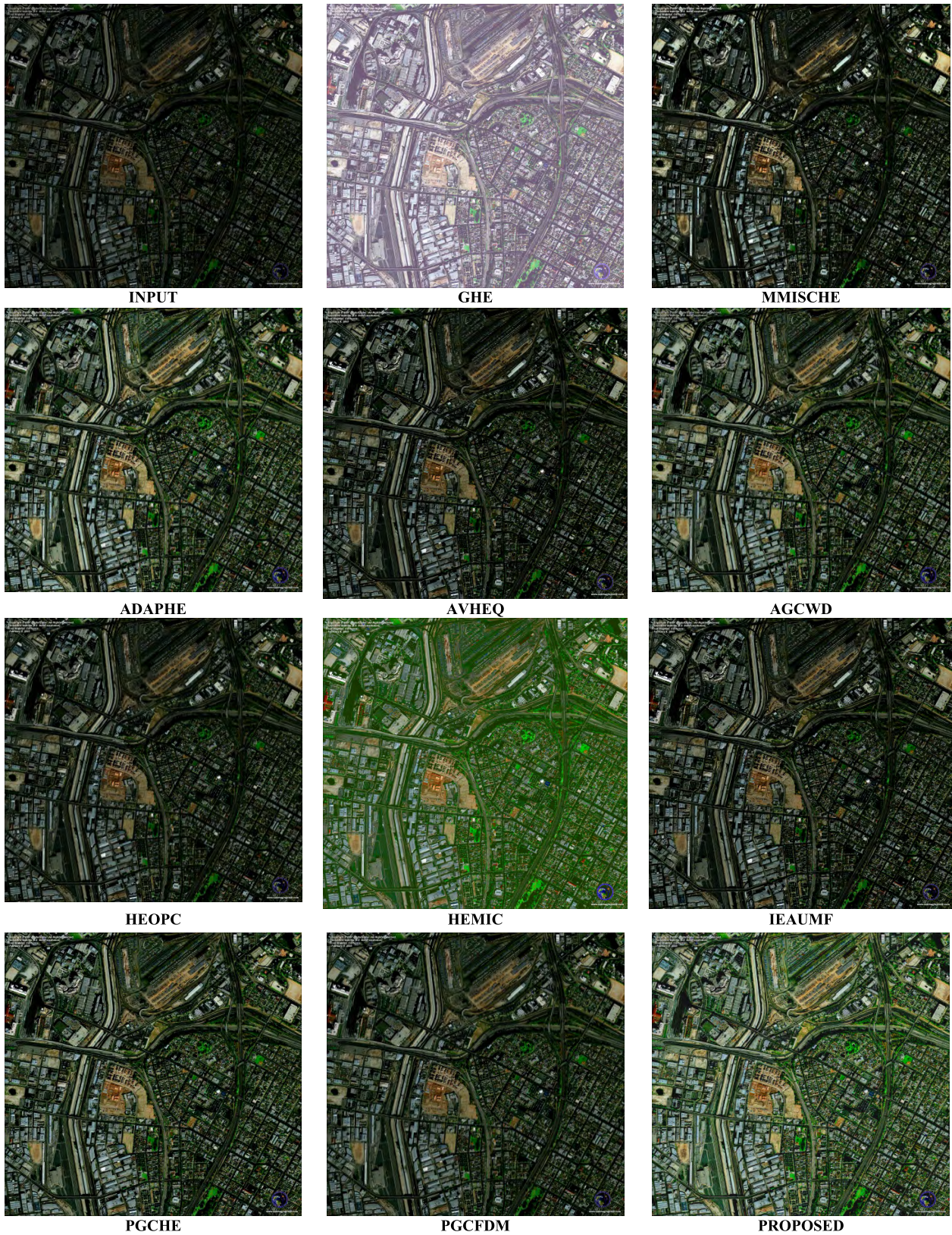


FIGURE 6. Visual presentation/ qualitative evaluation with comparison among input images; GHE; MMSICHE; ADAPHE; AVHEQ; AGCWD; HEOPC; HEMIC; IEAUMF; PGCHE; PGCDFM and the proposed approach for the image 6 (i.e., los angeles, california).

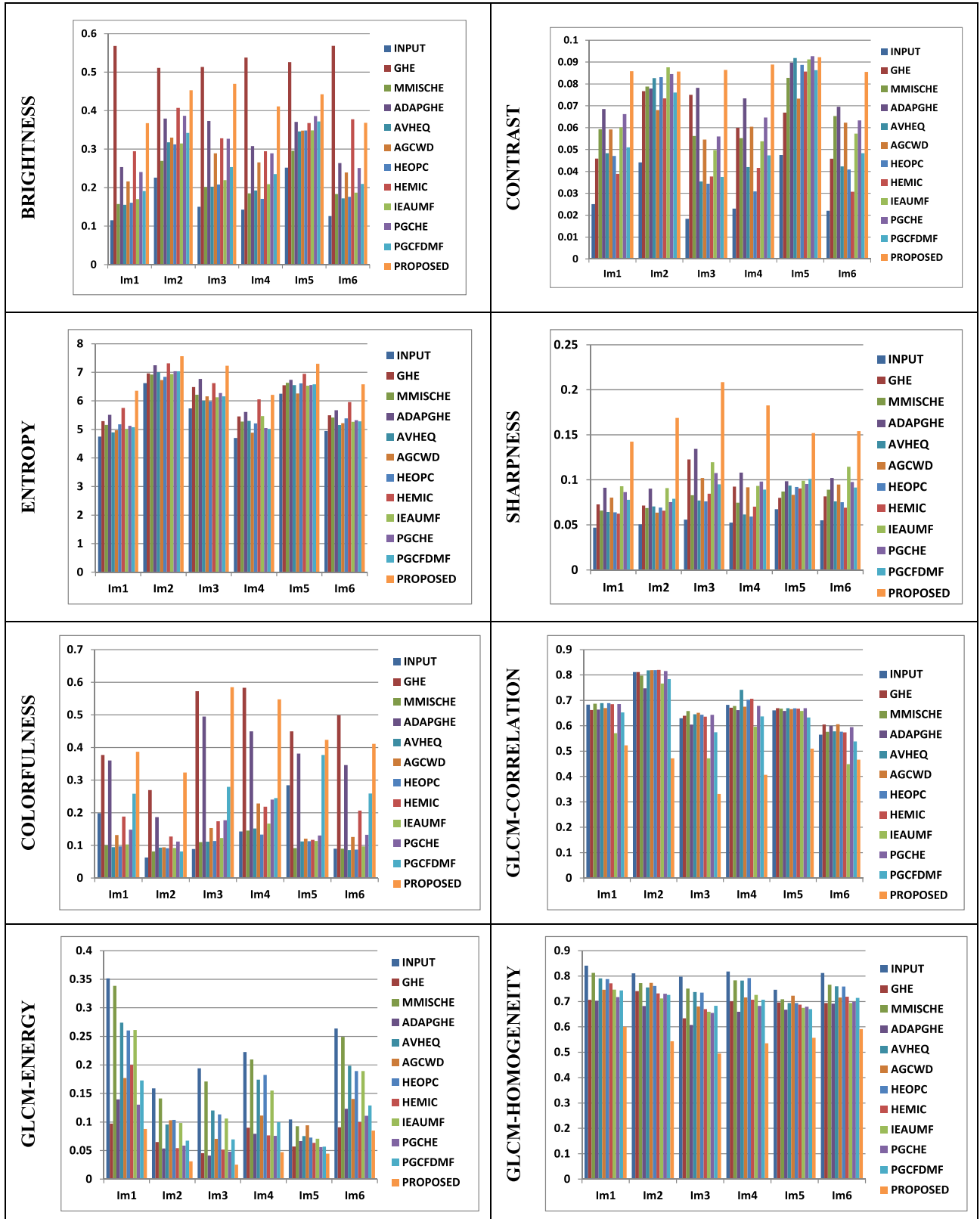


FIGURE 7. Comparative evaluation for performance indices for different test images (Im1 to Im6).

TABLE 2. Numerical results for comparative evaluation among input, GHE, MMSICHE, ADAPHE, AVHEQ, AGCWD, HEOPC, HEMIC, IEAUMF and the proposed approach by evaluating measures like brightness (B), CONTRAST (V), ENTROPY (H), SHARPNESS (S), COLORFULNESS (C), GLCM-CORRELATION (GC), GLCM-ENERGY (GE), GLCM-HOMOGENEITY (GH).

IMAGE No.	INDICES	INPUT	GHE	MMSICHE	ADAPHE	AVHEQ	AGCWD	HEOPC	HEMIC	IEAUMF	PGCHE	PGCFDM	Proposed
1.	B	0.1153	0.5681	0.1575	0.2534	0.1555	0.2164	0.1610	0.2947	0.1701	0.2407	0.1912	0.3675
	V	0.0251	0.0459	0.0593	0.0685	0.0483	0.0592	0.0471	0.0389	0.0601	0.0662	0.0510	0.0858
	H	0.0469	0.0728	0.0659	0.0913	0.0643	0.0802	0.0640	0.0625	0.0929	0.0864	0.0778	0.1424
	S	4.7471	5.2937	5.1580	5.5126	4.8985	4.9708	5.1778	5.7478	5.0058	5.1239	5.0781	6.3526
	C	0.1986	0.3770	0.1003	0.3602	0.0946	0.1318	0.0967	0.1882	0.1028	0.1481	0.2586	0.3870
	GC	0.8407	0.7066	0.8126	0.7029	0.7912	0.7461	0.7881	0.7714	0.7466	0.7174	0.7436	0.6000
	GE	0.3516	0.0972	0.3386	0.1397	0.2739	0.1770	0.2604	0.2001	0.2612	0.1302	0.1728	0.0878
GH	0.6831	0.6618	0.6864	0.6637	0.6891	0.6700	0.6891	0.6848	0.5706	0.6851	0.6523	0.5224	
2.	B	0.2261	0.5111	0.2693	0.3797	0.3179	0.3302	0.3126	0.4072	0.3146	0.3866	0.3421	0.4530
	V	0.0441	0.0767	0.0788	0.0779	0.0827	0.0681	0.0831	0.0734	0.0876	0.0845	0.0761	0.0857
	H	0.0506	0.0715	0.0686	0.0901	0.0704	0.0635	0.0692	0.0657	0.0908	0.0753	0.0790	0.1688
	S	6.6207	6.9598	6.9166	7.2433	7.0060	6.7278	6.8395	7.3162	6.9370	7.0363	7.0302	7.5627
	C	0.0627	0.2697	0.0815	0.1863	0.0932	0.0942	0.0913	0.1270	0.0922	0.1117	0.0812	0.3235
	GC	0.8108	0.7408	0.7724	0.6816	0.7552	0.7732	0.7608	0.7315	0.7119	0.7305	0.7255	0.5428
	GE	0.1589	0.0650	0.1413	0.0538	0.0956	0.1030	0.1037	0.0543	0.0982	0.0589	0.0672	0.0314
GH	0.8114	0.8113	0.7975	0.7473	0.8182	0.8195	0.8193	0.8201	0.7661	0.8156	0.7839	0.4713	
3.	B	0.1502	0.5135	0.2022	0.3731	0.2023	0.2892	0.2079	0.3281	0.2195	0.3271	0.2533	0.4699
	V	0.0184	0.0750	0.0562	0.0782	0.0354	0.0546	0.0344	0.0377	0.0498	0.0560	0.0375	0.0864
	H	0.0558	0.1227	0.0829	0.1345	0.0771	0.1021	0.0761	0.0846	0.1195	0.1075	0.0950	0.2085
	S	5.7321	6.4839	6.2171	6.7679	6.0040	6.1546	5.9817	6.6186	6.1216	6.2741	6.1538	7.2297
	C	0.0888	0.5724	0.1097	0.4949	0.1114	0.1534	0.1134	0.1739	0.1224	0.1773	0.2796	0.5848
	GC	0.7978	0.6336	0.7510	0.6072	0.7367	0.6802	0.7345	0.6700	0.6593	0.6547	0.6828	0.4952
	GE	0.1942	0.0454	0.1709	0.0412	0.1201	0.0704	0.1133	0.0515	0.1060	0.0480	0.0694	0.0254
GH	0.6292	0.6392	0.6578	0.6045	0.6451	0.6510	0.6434	0.6352	0.4714	0.6426	0.5743	0.3309	
4.	B	0.1430	0.5382	0.1852	0.3079	0.1925	0.2657	0.1708	0.2944	0.2093	0.2894	0.2354	0.4112
	V	0.0230	0.0600	0.0552	0.0734	0.0420	0.0604	0.0309	0.0416	0.0538	0.0646	0.0473	0.0889
	H	0.0525	0.0925	0.0745	0.1080	0.0616	0.0917	0.0592	0.0703	0.0932	0.0981	0.0892	0.1827
	S	4.6992	5.4557	5.2727	5.6113	5.2968	4.8846	5.2115	6.0543	5.4682	5.0509	5.0158	6.2101
	C	0.1426	0.5829	0.1452	0.4494	0.1519	0.2287	0.1332	0.2189	0.1670	0.2401	0.2448	0.5474
	GC	0.8180	0.7005	0.7830	0.6598	0.7822	0.7161	0.7924	0.7070	0.7253	0.6822	0.7069	0.5351
	GE	0.2227	0.0901	0.2097	0.0793	0.1742	0.1114	0.1824	0.0767	0.1550	0.0758	0.0995	0.0472
GH	0.6823	0.6708	0.6777	0.6614	0.7414	0.6749	0.7024	0.7064	0.5959	0.6781	0.6364	0.4065	
5.	B	0.2520	0.5259	0.2959	0.3711	0.3461	0.3480	0.3486	0.3679	0.3490	0.3859	0.3721	0.4426
	V	0.0475	0.0669	0.0828	0.0897	0.0918	0.0733	0.0887	0.0857	0.0912	0.0927	0.0863	0.0922
	H	0.0673	0.0800	0.0871	0.0984	0.0935	0.0832	0.0921	0.0905	0.0990	0.0953	0.1010	0.1520
	S	6.2499	6.5434	6.6297	6.7393	6.5505	6.2553	6.6110	6.9469	6.5278	6.5582	6.5771	7.3002
	C	0.2839	0.4493	0.0915	0.3813	0.1122	0.1206	0.1126	0.1167	0.1134	0.1305	0.3772	0.4234
	GC	0.7462	0.6960	0.7088	0.6675	0.6935	0.7225	0.6938	0.6874	0.6748	0.6791	0.6700	0.5569
	GE	0.1044	0.0572	0.0926	0.0664	0.0754	0.0942	0.0727	0.0635	0.0709	0.0561	0.0570	0.0447
GH	0.6606	0.6690	0.6672	0.6584	0.6691	0.6654	0.6683	0.6676	0.6584	0.6690	0.6322	0.5091	
6.	B	0.1265	0.5684	0.1833	0.2637	0.1719	0.2393	0.1761	0.3776	0.1871	0.2512	0.2095	0.3682
	V	0.0220	0.0458	0.0653	0.0696	0.0423	0.0623	0.0409	0.0307	0.0573	0.0633	0.0483	0.0855
	H	0.0551	0.0816	0.0890	0.1020	0.0761	0.0949	0.0751	0.0690	0.1146	0.0976	0.0914	0.1542
	S	4.9446	5.4939	5.4127	5.6706	5.1541	5.2182	5.3898	5.9595	5.2632	5.3252	5.2787	6.5802
	C	0.0900	0.4987	0.0896	0.3462	0.0855	0.1259	0.0872	0.2064	0.0966	0.1322	0.2589	0.4109
	GC	0.8119	0.6938	0.7655	0.6913	0.7598	0.7155	0.7583	0.7182	0.6939	0.6988	0.7140	0.5910
	GE	0.2637	0.0909	0.2491	0.1232	0.1984	0.1405	0.1894	0.0995	0.1893	0.1108	0.1291	0.0849
GH	0.5649	0.6051	0.5762	0.5993	0.5779	0.6061	0.5769	0.5737	0.4489	0.5948	0.5381	0.4663	

where, $\Delta_{rg}, \Delta_{yb}, \mu_{rg}, \mu_{yb}, \sigma_{rg}, \sigma_{yb}$, symbolizes corresponding differential values, differential mean and corresponding differential standard deviation values, respectively.

C. GLCM BASED PERFORMANCE INDICES

Spatial co-occurrence of the image pixels are usually avoided while evaluating the intensity based indices, and hence, to resolve it, Gray-Level Co-occurrence Matrix based performance indices also plays a significant role for texture

and other spatially influenced properties. Overall statistical and spatial behavior w.r.t. reference pixel can be derived by calculating the pixel-wise average for all four directional matrices:

$$GLCM = 0.25 \left(GLCM_0 + GLCM_{\pi/4} + GLCM_{\pi/2} + GLCM_{3\pi/4} \right); \tag{27}$$

TABLE 3. Statistical improvement achieved for various quality measures (averaged over 30 images).

	Brightness	Contrast	Entropy	Sharpness	Colorfulness	Correlation	Energy	Homogeneity
Input	0.1689	0.0300	0.0547	5.4989	0.1444	0.8042	0.2159	0.6719
Output	0.3890	0.0757	0.1353	6.7521	0.4281	0.5982	0.0594	0.5257
Increment	130.4%	152.4%	147.3%	22.8%	196.4%	-25.6%	-72.5%	-21.8%

In this paper, three well known GLCM based indices, i.e. GLCM-Correlation, GLCM-Energy and GLCM-Homogeneity are evaluated. Any element of the GLCM matrix $\Psi(m, n)$, is usually evaluated by considering the n^{th} neighboring pixel w.r.t. m^{th} pixel, and later on, by calculating the $\mu_m, \mu_n, \sigma_m,$ and σ_n as the corresponding mean values and standard deviation values respectively. GLCM-correlation (GC) stands for the interdependency for the corresponding neighborhood of the pixels w.r.t. reference pixels, expressed as:

$$GC = \sum_{m=0}^{M-1} \sum_{n=0}^{N-1} \frac{(m - \mu_m)(n - \mu_n) \Psi(m, n)}{\sigma_m \cdot \sigma_n}, \quad (28)$$

GLCM-Energy (GE) can be characterized by normalized count of repeated pairs. Intuitively, these are responsible for uniformity of texture, and hence, expressed as:

$$GLCM - Energy (GE) = \sum_{m=0}^{M-1} \sum_{n=0}^{N-1} \Psi(m, n)^2, \quad (29)$$

GLCM-homogeneity (GH) can be characterized by the closeness of neighboring pixels with reference pixels. Intuitively, these are also responsible for uniformity of texture, and hence, expressed as:

$$GH = - \sum_{m=0}^{M-1} \sum_{n=0}^{N-1} \Psi(m, n) \log_2 \Psi(m, n), \quad (30)$$

Ideally, all these values should be as low as possible for better texture visualization of the content. Hence, relatively lower values for these parameters are usually appreciated.

D. COMPARATIVE ASSESSMENT OF THE PROPOSED PGC-RLFOIM

Overall assessment of the proposed approach is done by rigorous experimentation by evaluating all above-mentioned performance indices for some of the earlier, state-of-the-art proposals by various researchers. The tabular results along with the resulted images and their corresponding bar statistics are produced here for portraying the general excellence of the proposed approach. Individual results can be easily analyzed by considering the core objective of simultaneous contrast and entropy improvement along with sharpness enhancement. In addition to it, some amount of brightness improvement is also desired in case of the dark images, and in this way more scope can be explored for further contrast improvement by exploring more span of intensity levels. For accounting GLCM-based assessment, as discussed

above, the least values of indices like GLCM correlation (GC), GLCM energy (GE) and GLCM-homogeneity (GH) are appreciated for a quality enhanced image. The theoretical excellence due to the presence of OBL is quite implacable, and hence can be accepted easily for the outperformance of the proposed method due to its self-ignited, exhaustive learning mechanism. It can be proved experimentally by integrating various optimization methods along with hereby proposed PGCRLFOIM framework by utilizing the comparable resources like the same iteration-count along with same population size; so that the unbiased comparison can be illustrated for the various algorithms' co-existence compatibility. OBL-SCA is utilized for final modeling, which itself has been derived by imparting intelligence based on opposition based exhaustive machine learning approach; and hence, termed as OBL-SCA.

Clustered bar-graphs as presented in Fig. 7 also draw a very clear sketch for the outperformance of the proposed approach. The performance bar graphs for six different test-images are plotted. The different colors of the bar columns represent different test images. Better quality improvement can be easily advocated by increased value for brightness (B), contrast (V), entropy (H), sharpness (S) and colorfulness (C) as shown in Fig 7. (a-e). Contrary to this, decreased values of GLCM-based indices namely correlation (R), energy (E) and homogeneity (M) collectively advocate the better texture based quality improvement, as shown in Fig 7(f-h). As listed in Table 3, an averaged analysis is also presented over various test images. Accordingly, 152.4% increment (2.52 times) is achieved over the input contrast along with the simultaneous 147.3% (2.47 times) increment in the discrete entropy level and 22.8% (1.228 times) increment in the sharpness content. Also, for dark color images, higher values of brightness and colorfulness are also desired, those are reported with 130.4% (2.3 times) and 196.4% (2.96 times) increased w.r.t. the input indices, respectively. In addition, the textural improvement is advocated in terms of desired comparative reduction of GLCM based metrics, namely correlation, energy and homogeneity are suppressed by 25.6% (0.744 times), 72.5% (0.275 times), and 21.8% (0.782 times), respectively. Hence, the desired objective is achieved efficiently.

V. CONCLUSION

As a concluding note, it can be said that the prime objective is to extract more and more information by imparting adaptive/content-wise boosting/improvement for visual features of the poorly acquired, remotely sensed textured satel-

lite images. Along with proper illumination improvement for dark satellite images, content dependent texture enhancement is also required for efficient post-processing usage. With this above-mentioned objective, an optimal fusion based framework is proposed for a constructive association of gamma-compressed and gamma-expanded intensity channels, with a third channel which is a novel inclusion in this paper. This third channel is a texture enhanced version of the image obtained by fractional-order RL integration based adaptive 2-D filtering. Effectively proposed, 2-D RL fractional-order integral mask is a highly efficient version of blurring/smoothing filter and when, thus processed filtered output is negatively augmented with input intensity channel, with proper intensity dependent scaling factor, leads to texture enhanced version of the input channel. The proposed PGC-RLFOIM approach can also be identified as a weighted association of all three interim channels, namely gamma compressed, gamma expanded, and the fractional-order integration based texture enhanced version. Optimal association of these interim images is planned in an intelligent manner by adaptive exploration along with efficient garnering of missing intensity levels throughout the span of permissible intensity levels. Along with this newly proposed fusion framework, a novel fitness function has been also suggested in this paper which seems very robust for all kinds of textural and non-textural image details. According to the demand, OBL-SCA is associated with the proposed framework after rigorous experimentation, so that a four-dimensional (4-D) search space can be fruitfully explored and exploited for achieving the suitable values of $(\alpha, \beta, \gamma, \nu)$ so that overall enhancement can be imparted. The approach has been found very efficient for remotely sensed satellite images and on some general images as well.

REFERENCES

- [1] J. Wang, Y. Ye, X. Pan, X. Gao, and C. Zhuang, "Fractional zero-phase filtering based on the Riemann–Liouville integral," *Signal Process.*, vol. 98, pp. 150–157, May 2014. doi: [10.1016/j.sigpro.2013.11.024](https://doi.org/10.1016/j.sigpro.2013.11.024).
- [2] Y.-F. Pu, J.-L. Zhou, and X. Yuan, "Fractional differential mask: A fractional differential-based approach for multiscale texture enhancement," *IEEE Trans. Image Process.*, vol. 19, no. 2, pp. 491–511, Feb. 2010. doi: [10.1109/TIP.2009.2035980](https://doi.org/10.1109/TIP.2009.2035980).
- [3] H. Singh, A. Kumar, L. K. Balyan, and G. K. Singh, "A novel optimally weighted framework of piecewise gamma corrected fractional order masking for satellite image enhancement," *Comput. Elect. Eng.*, to be published. doi: [10.1016/j.compeleceng.2017.11.014](https://doi.org/10.1016/j.compeleceng.2017.11.014).
- [4] H. Singh, A. Kumar, L. K. Balyan, and G. K. Singh, "Swarm intelligence optimized piecewise gamma corrected histogram equalization for dark image enhancement," *Comput. Elect. Eng.*, vol. 70, pp. 462–475, Aug. 2018. doi: [10.1016/j.compeleceng.2017.06.029](https://doi.org/10.1016/j.compeleceng.2017.06.029).
- [5] K. Singh and R. Kapoor, "Image enhancement via median-mean based sub-image-clipped histogram equalization," *Opt.-Int. J. Light Electron Opt.*, vol. 125, no. 17, pp. 4646–4651, Sep. 2014. doi: [10.1016/j.ijleo.2014.04.093](https://doi.org/10.1016/j.ijleo.2014.04.093).
- [6] K. Zuiderveld, "Contrast limited adaptive histogram equalization," in *Graphics Gems IV*, P. Heckbert, Ed. New York, NY, USA: Academic, 1994. doi: [10.1016/B978-0-12-336156-1.50061-6](https://doi.org/10.1016/B978-0-12-336156-1.50061-6).
- [7] S. C.-F. Lin et al., "Image enhancement using the averaging histogram equalization (AVHEQ) approach for contrast improvement and brightness preservation," *Comput. Elect. Eng.*, vol. 46, pp. 356–370, Aug. 2015. doi: [10.1016/j.compeleceng.2015.06.001](https://doi.org/10.1016/j.compeleceng.2015.06.001).
- [8] S.-C. Huang, F.-C. Cheng, and Y.-S. Chiu, "Efficient contrast enhancement using adaptive gamma correction with weighting distribution," *IEEE Trans. Image Process.*, vol. 22, no. 3, pp. 1032–1041, Mar. 2013. doi: [10.1109/TIP.2012.2226047](https://doi.org/10.1109/TIP.2012.2226047).
- [9] H. Singh, A. Kumar, L. K. Balyan, and G. K. Singh, "Slantlet filter-bank-based satellite image enhancement using gamma-corrected knee transformation," *Int. J. Electron.*, vol. 105, no. 10, pp. 1695–1715, 2018. doi: [10.1080/00207217.2018.1477199](https://doi.org/10.1080/00207217.2018.1477199).
- [10] C. Y. Wong et al., "Histogram equalization and optimal profile compression based approach for colour image enhancement," *J. Vis. Commun. Image Represent.*, vol. 38, pp. 802–813, Jul. 2016. doi: [10.1016/j.jvcir.2016.04.019](https://doi.org/10.1016/j.jvcir.2016.04.019).
- [11] C. Y. Wong et al., "Image contrast enhancement using histogram equalization with maximum intensity coverage," *J. Mod. Opt.*, vol. 63, no. 16, pp. 1618–1629, 2016. doi: [10.1080/09500340.2016.1163428](https://doi.org/10.1080/09500340.2016.1163428).
- [12] S. C.-F. Lin et al., "Intensity and edge based adaptive unsharp masking filter for color image enhancement," *Optik*, vol. 127, no. 1, pp. 407–414, 2016. doi: [10.1016/j.ijleo.2015.08.046](https://doi.org/10.1016/j.ijleo.2015.08.046).
- [13] J. Kennedy and R. Eberhart, "Particle swarm optimization," in *Proc. IEEE Int. Conf. Neural Netw.*, vol. 4, Nov. 1995, pp. 1942–1948. doi: [10.1109/ICNN.1995.488968](https://doi.org/10.1109/ICNN.1995.488968).
- [14] D. Karaboga and B. Basturk, "On the performance of artificial bee colony (ABC) algorithm," *Appl. Soft Comput.*, vol. 8, pp. 687–697, Jan. 2008. doi: [10.1016/j.asoc.2007.05.007](https://doi.org/10.1016/j.asoc.2007.05.007).
- [15] X. S. Yang and S. Deb, "Cuckoo search via Lévy flights," in *Proc. World Congr. Nature Biol. Inspired Comput. (NABIC)*, Dec. 2009, pp. 210–214. doi: [10.1109/NABIC.2009.5393690](https://doi.org/10.1109/NABIC.2009.5393690).
- [16] S. Mirjalili, "SCA: A sine cosine algorithm for solving optimization problems," *Knowl.-Based Syst.*, vol. 96, pp. 120–133, Mar. 2016. doi: [10.1016/j.knsys.2015.12.022](https://doi.org/10.1016/j.knsys.2015.12.022).
- [17] M. A. Elaziz, D. Oliva, and S. Xiong, "An improved opposition-based sine cosine algorithm for global optimization," *Expert Syst. Appl.*, vol. 90, pp. 484–500, Dec. 2017. doi: [10.1016/j.eswa.2017.07.043](https://doi.org/10.1016/j.eswa.2017.07.043).
- [18] [Online]. Available: <https://www.satimagingcorp.com/gallery/quickbird/>
- [19] [Online]. Available: <https://www.satimagingcorp.com/gallery/pleiades-1/>
- [20] [Online]. Available: <https://www.satimagingcorp.com/gallery/pleiades-2/>



HIMANSHU SINGH received the B.E. degree (Hons.) in electronics and communication engineering from the Madhav Institute of Technology and Science, Gwalior, India, in 2010. He is currently pursuing the Ph.D. degree in electronics and communication engineering with the Indian Institute of Information Technology, Design and Manufacturing Jabalpur, India. His research interests include signal and image processing applications, image enhancement, and soft-computing techniques.



ANIL KUMAR received the B.E. degree in electronic and telecommunication engineering from the Army Institute of Technology, Pune University, India, in 2002, and the M.Tech. and Ph.D. degrees in electronic and telecommunication engineering from IIT Roorkee, India, in 2006 and 2010, respectively. He is currently an Assistant Professor with the Electronic and Communication Engineering Department, Indian Institute of Information Technology, Design and Manufacturing, Jabalpur, India.

He is also a Visiting Researcher with the Gwangju Institute of Science and Technology, South Korea. His research interests include design of digital filters and filter bank, biomedical signal processing, image processing, and speech processing.



L. K. BALYAN received the M.Sc. degree in applied mathematics from IIT Roorkee and the Ph.D. degree in applied mathematics from IIT Kanpur, in 2009. He is currently an Assistant Professor of mathematics with the Discipline of Natural Science, IIITDM, Jabalpur. His research interests include numerical solution of partial differential equations, and spectral methods and their applications.



HEUNG-NO LEE received the B.S., M.S., and Ph.D. degrees in electrical engineering from the University of California, Los Angeles, CA, USA, in 1993, 1994, and 1999, respectively. From 1999 to 2002, he was a Research Staff Member with HRL Laboratories, LLC, Malibu, CA, USA. From 2002 to 2008, he was an Assistant Professor with the University of Pittsburgh, PA, USA. In 2009, he joined the School of Electrical Engineering and Computer Science, Gwangju Institute of Science and Technology, South Korea, where he currently holds a position. His areas of research include information theory, signal processing theory, communications/networking theory, and their application to wireless communications and networking, compressive sensing, the future Internet, and brain-computer interface.

• • •